
Article:
Bui, T-T, Limam, A and Sarhosis, V orcid.org/0000-0002-5748-7679 (2021) Failure analysis of masonry wall panels subjected to in-plane and out-of-plane loading using the discrete element method. European Journal of Environmental and Civil Engineering, 25 (5). pp. 876-892. ISSN 2116-7214

https://doi.org/10.1080/19648189.2018.1552897

Failure analysis of masonry wall panels subjected to in-plane and out-of-plane loading using the discrete element method

T. T. Bui[1], A. Limam[2], V. Sarhosis[3]

[1]*University of Lyon, INSA Lyon, GEOMAS, France, tan-trung.bui@insa-lyon.fr*

[2]*University of Lyon, France, ali.limam@insa-lyon.fr*

[3]*School of Engineering, Newcastle University, Newcastle, UK, vasilis.sarhosis@newcastle.ac.uk*

Abstract

This paper aims to evaluate the ability of the Discrete Element Method (DEM) to accurately predict the mechanical behavior of modern brickwork and concrete block masonry wall panels subjected to in-plane and out-of-plane loading. The efficiency of the DEM is based on the suitability of the DEM models to predict the development and propagation of cracks up to collapse, the associated stress distributions and the ultimate load carrying capacity of masonry wall panels subjected to external loading. Numerical results are compared with experimental ones obtained from large-scale tests carried out in the laboratory. A good agreement between the numerical and the experimental results obtained which confirms the efficiency and robustness of the DEM to simulate the in-plane and out-of-plane non-linear behavior of modern masonry wall panels with sufficient accuracy. Moreover, a collection of verified material parameters is provided to be used by other researchers and engineers to develop reliable computational models and understand the mechanical behavior of masonry structures. Finally, computational results from this study can help prevent engineering failures and provide reference for stakeholders devising strategies for improving risk management and disaster prevention in masonry structures.

Keywords: masonry, discrete element method, in-plane loading, out of plane loading, wall

1 Introduction

Masonry is a brittle, anisotropic, composite material that exhibits distinct directional properties due to the mortar joints which act as planes of weakness. When masonry is subjected to very low levels of stress, it behaves in a linear elastic manner. However, the behavior of masonry is characterized by high non-linearity after the formation of cracks and the subsequent redistribution of stresses through the uncracked material as the structure approaches to collapse. Research is needed to be able to understand the in-plane and out of plane behaviour of masonry construction subjected to external loading. In particular, it is important to understand the pre- and post-cracking behaviour and decide on the need for repair and/or strengthening. As experimental research is prohibitively expensive, it is fundamentally important to have a computational model available that can be used to predict the in-service and near-collapse behaviour with sufficient accuracy. Such model can then be used to investigate a range of complex problems and scenarios that would not, otherwise, be possible.

According to Lourenço (1996), numerical models able to simulate the mechanical behavior of masonry can be classified into two major categories. These are: a) micro-models including detailed micro-models and simplified micro-models; and b) macro-models. Micro-models consider the various components which result in an accurate representation of the structure. Generally, such modelling approach is limited due to large calculation time required for a structural element to be analyzed. Also, the micro-modelling approach is commonly used when parts of a structure are to be modelled. On the other hand, at the macro-scale, models are relatively simple to use and require fewer input data. The macro-models are generally based on the use of homogenization techniques. Overall, the micro-modelling approach represents more accurately and rigorously the mechanical behavior of masonry structures.

A wide variety of numerical methods are available to simulate the mechanical behavior of masonry structures and these can be classified into two main groups: a) Continuous models; and b) Discrete models. Continuous models are based on the continuum mechanics. The Finite Element Method (FEM) and the Boundary-Element Method (BEM) are typical examples of these approaches. The macro-modelling strategy is well suited for these continuous models. Developments in the plasticity theory have assisted significantly to mature these approaches (Lourenço, 1996; Lourenço, 2000). Within macro-models, cracking is represented by a “smeared-crack” approach. Macro-models were initially developed by Rots et al. (1985) for the design of concrete structures. The “smeared-crack” approach takes into account the crack effect, which induces relaxation in stress of the material, via negative softening or hardening. The "smeared-crack" approach was later extended to masonry structures by Lofti et al. (1991). The approach is

controlled by combining fracture energy to the element size. A drawback of the approach is that complete separation between masonry components (i.e. blocks) cannot be achieved. Moreover, when modelling masonry structures, this approach is highly dependent on the size of the mesh used in the development of the model. Lourenço and Rots (1997) developed models based on the FEM with interface elements to simulate the in-plane mechanical behavior of masonry walls. For an overview of the different computational methods used to simulate the mechanical behaviour of unreinforced masonry structures, the reader can be directed to Moradabadi and Laefer (2014).

Discrete element method (DEM) has its origin in the early 1970s. It was initially used to simulate progressive rock movement using rigid block assemblies in two dimensions (Cundall 1971a, 1971b). The method was later extended to predict the mechanical behavior of masonry structures (Munjiza, 2004; Lemos, 2007; Bui, 2014a; Sarhosis 2012; Sarhosis and Lemos 2018; Forgács et al. 2017; Bui et al. 2017). Within DEM, the heterogeneous nature of the masonry is taken into account explicitly. In this way, the discontinuity of interfaces between masonry units/blocks can be described. So far, numerical models based on the DEM have been mainly applied to masonry structures where failure is predominantly induced by mechanisms in which the block deformability is limited or has no role at all (Sarhosis et al. 2014a; Sarhosis et al. 2015; Forgács et al. 2018). According to the method, masonry blocks can be represented as an assembly of rigid or deformable blocks which may take any arbitrary geometry. Rigid blocks do not change their geometry as a result of any applied loading. Deformable blocks are internally discretised into finite difference triangular zones. These zones are continuum elements as they occur in the finite element method (FEM). Mortar joints are represented as zero thickness interfaces between the blocks. Representation of the contacts between blocks is not based on joint elements, as it occurs in the discontinuous finite element models. Instead, the contact is represented by a set of point contacts, with no attempt to obtain a continuous stress distribution through the contact surface. The assignment of contacts allows the interface constitutive relations to be formulated in terms of the stresses and relative displacements across the joint. As with FEM, the unknowns are the nodal displacements and rotations of the blocks. However, unlike FEM, the unknowns in DEM are solved explicitly by differential equations from the known displacement, while Newton's second law of motion gives the motion of the blocks resulting from known forces acting on them. So, large displacements and rotations of the blocks are allowed with the sequential contact detection and update of tasks automatically. This differs from FEM, where the method is not readily capable of updating the contact size or creating new contacts. DEM is also applicable for quasi-static problems using artificial viscous damping controlled by an adaptive algorithm. In view of the diversity and

complexity of non-linear behavior observed across the masonry structures, the validation of discrete modeling remains a crucial task.

To date, many researchers have investigated the mechanical behaviour of masonry subjected to in-plane loading; simply because masonry structures are designed to withstand in-plane vertical load. However, not much research has been undertaken on the mechanical behavior of masonry subjected to out-of-plane loading. The flexural strength of masonry was represented mainly in relation to the resistance of walls to withstand wind load effects (Sarhosis et al 2014b). However, out-of-plane bending in masonry walls can also occure due to:

a) natural disasters such as earthquakes and floods (Kelman, 2003);

b) snow avalanches and mud after a landslide (Colas, 2009);

c) accidental damages such as the explosions inside buildings (Thomas, 1971);

d) accidental impacts like vehicle hitting a wall of a building (Kelman, 2003); and

e) terrorist attacks.

The aim of this paper is to evaluate the efficiency of the DEM to accurately predict the mechanical behavior of different brickwork and blockwork masonry wall panels subjected to external in-plane and out-of-plane loading. The commercial three-dimensional software 3DEC developed by Itasca has been used in this study (Itasca, 2018). The efficiency of the DEM was assessed based on the suitability of the model to predict the development and the propagation of cracks up to collapse, the associated stress distributions in the wall panels at the different magnitude of applied loading and the ultimate load bearing capacity. Numerical results were compared to experimental ones from testing full-scale masonry wall panels in the laboratory. Moreover, a collection of verified material parameters is provided.

2 Overview of the Discrete Element Method for modelling masonry

The three-dimensional numerical code 3DEC based on the DEM, and developed by Itasca, has been used in this study. Within 3DEC, the domain is represented as an assemblage of rigid or deformable discrete blocks (brick or concrete masonry units) connected together by zero thickness interfaces representing mortar joints. In masonry structures, damage is often consecrated in the mortar joints rather than the masonry units (Bui et al., 2017). Within DEM, masonry units can be represented as rigid blocks. Rigid blocks does not change their geometry as a result of any applied loading. Rigid blocks are able to undergo only translational and rotational motion; which reduces significantly the computational time required to run the numerical simulations. Deformable blocks are internally discretised into finite number of constant strain tetrahedral elements (Lemos, 2007). These zones are continuum elements, as in the finite element method (FEM). However, unlike

FEM, in DEM, a compatible finite element mesh between the blocks and the joints is not required. So, large displacements and rotations of the blocks are allowed with the sequential contact detection and update of tasks automatically. This differs from FEM where the method is not readily capable of updating the contact size or creating new contacts. Despite these advantages, comparatively to FEM, the diversity and complexity of non-linear behavior observed across the masonry structures subjected to external loads necessitates careful validations.

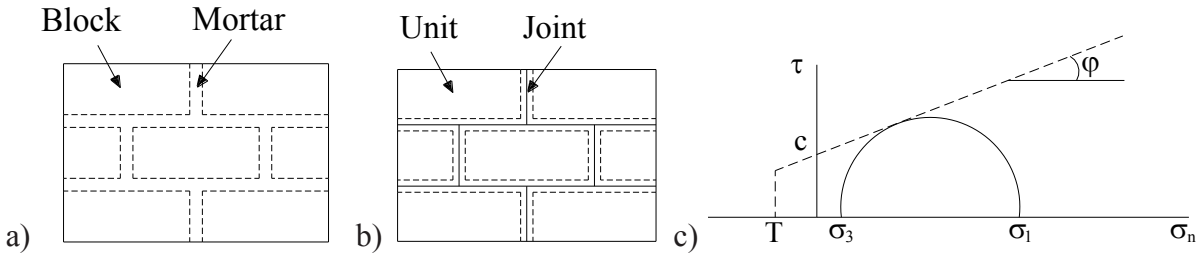

Figure 1: a) Detailed micro-modelling masonry wall; b) Simplified micro-modelling masonry wall; c) Mohr-Coulomb model of joint with tension cut-off.

a) Representation of the mortar joint interface

Within DEM, mortar joints are represented as zero-thickness interfaces, while the units are slightly expanded in size in order to keep the geometry of the structure unchanged (Figure 1b). In this way, it is possible to consider masonry as a set of blocks bonded together by potential fracture slip lines at the mortar joints. Several researchers, including Andreaus et al, (1999a & b), have studied the interaction of masonry blocks using the classical simple Coulomb constitutive model, characterized with only three input parameters including: a) the normal stiffness; b) the shear stiffness; and c) the friction angle. However, today, there are advanced models developed in which take into account the frictional resistance, the tensile and shear-bond strength too. Such models also consider a representative fracture energy as well as they avoid numerical perturbations that may be induced by sudden bond failure (Sarhosis 2012; Sarhosis & Sheng 2014; Lemos 2007; Giamundo et al. 2014). Interaction between the blocks is enabled based on constitutive relationships such as the Mohr-Coulomb with a tension cut-off (Figure 1a). This interface constitutive model considers apart from dilation, both shear and tensile failure. In the elastic range, the behavior is governed by normal and shear stiffness of the interfaces k_n and k_s according to:

$$\{\sigma\} = [K]\{u\} \quad \text{or} \quad \begin{Bmatrix} \tau_s \\ \sigma_n \end{Bmatrix} = \begin{bmatrix} k_s & 0 \\ 0 & k_n \end{bmatrix} \begin{bmatrix} u_s \\ u_n \end{bmatrix} \tag{1}$$

where σ_n is the normal loading; u_n is the normal displacement; τ_s is the shear stress; and u_s is the shear displacement. The maximum shear force is given by Equation (2):

$$\tau_{max} = c + \sigma_{n(max)} \cdot \tan\varphi \quad (2)$$

where c and φ are the interface cohesion and friction angle accordingly. When shear strength is reached, it drops until a residual strength is achieved (Figure 2a). The residual shear strength (τ_{res}) can be calculated from Equation (3):

$$\tau_{res} = \sigma_{n(max)} \cdot \tan\varphi \quad (3)$$

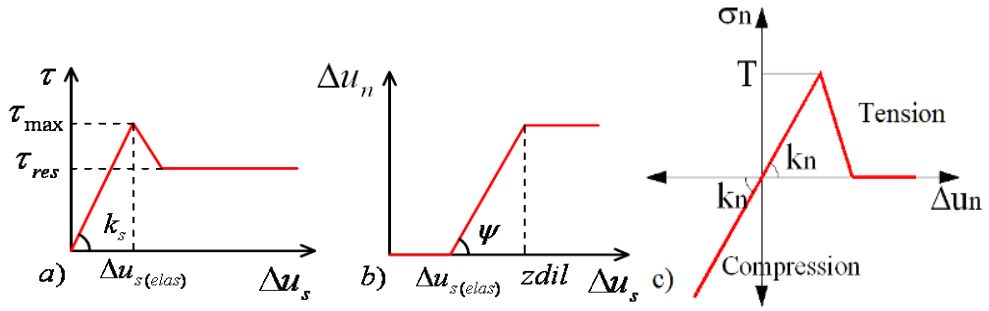

Figure 2: Representation of the interface behaviour: a) Mohr-Coulomb slip model; b) Bilinear dilatant model; c) Behavior under uniaxial loading.

From Figure 2b, the interface begins to dilate when it fails in shear, at shear displacement $\Delta u_{s(elas)}$. The dilation (ψ) can then be estimated from Equation (4):

$$\Delta u_{n,dilatation} = \Delta u_s \tan\psi \quad (4)$$

where $\Delta u_{n,dilatation}$ is the normal displacement and Δu_s is the shear displacement. Also, the normal stress ($\sigma_{n,total}$) can be adjusted to take into account the effect of dilatation:

$$\sigma_{n,total} = \sigma_{n,elastic} + \sigma_{n,dilatation} = k_n.\Delta u_n + k_n.\Delta u_{n,dilatation} \quad (5)$$
$$= k_n.\Delta u_n + k_n.\Delta u_s \tan\psi$$

where $\sigma_{n,elastic}$ is the elastic normal stress, $\sigma_{n,dilatation}$ is the normal stress due to dilation, k_n and k_s is the normal and shear stiffnesses, Δu_n is the change in normal displacement, $\Delta u_{n,dilatation}$ is the change in normal displacement as a result of the dilation, and Δu_s is the change in shear displacement. In the present f dilation, the shear displacement is in the plastic phase ($\Delta u_s > \Delta u_{s(elas)}$, Figure 2a). The normal displacement is assumed linear until a value equal to Z_{dil} is reached (Figure 2b). If shear displacement increments are in the same direction as the total shear displacement, then dilatation angle increases. However, if the shear increments are in the opposite direction, dilation

angle decreases. The interface behavior under uniaxial loads is shown in Figure 2c, where T is the interface tensile strength. Before the tensile failure ($\sigma_n < T$) is achieved, an elastic behavior is assumed.

b) Representation of the masonry block units

Masonry block units can behave as linear elastic or elasto-plastic based on the Mohr-Coulomb criterion. The Mohr-Coulomb criterion is expressed in terms of the principal stresses σ_1, σ_2, and σ_3, which constitute the three components of the generalized stress vector (n = 3), whereby for the three principal stresses, it must satisfy: $\sigma_1 \leq \sigma_2 \leq \sigma_3$. Components of the corresponding generalized strain vector are the principal strains ε_1, ε_2, ε_3. This criterion can be represented in the plane (σ_1, σ_3), as illustrated in Figure 3 (compressive stresses are negative). The failure envelope (f) (σ_1, σ_3) = 0 is defined from point A to B by the Mohr-Coulomb shear failure criterion $f^s = 0$ with $f^s=\sigma_1 - \sigma_3 N_\varphi + 2c\sqrt{N_\varphi}$; and from B to C by a tensile failure criterion as per $f^t = 0$ with $f^t = \sigma_3 - \sigma_t$; where φ is the friction angle, c is the cohesion, σ_t is the tensile strength, and $N_\varphi = \frac{1+\sin\varphi}{1-\sin\varphi}$.

The tensile strength of the material cannot exceed the value of σ_3 corresponding to the intersection point of the straight lines $f^s = 0$ and $\sigma_1 = \sigma_3$ in the (σ_1, σ_3) plane. The maximum stress (σ^t_{max}) is given by:

$$\sigma^t_{max} = \frac{c}{\tan\varphi} \qquad (6)$$

The potential function, g^s, used to define the shear plastic flow, corresponds to a non-associated law according to the equation $g^s = \sigma_1 - \sigma_3 N_\psi$, where ψ is the dilation angle and $N_\Psi = \frac{1+\sin\psi}{1-\sin\psi}$.

If the shear failure takes place, the stress point is placed on the curve $f^s = 0$ using a flow law which is derived by using the potential function g^s. If tensile failure is reached, the new stress point is simply reset to satisfy the relationship f^t equal to zero (Figure 3) and no flow rule is used in this case.

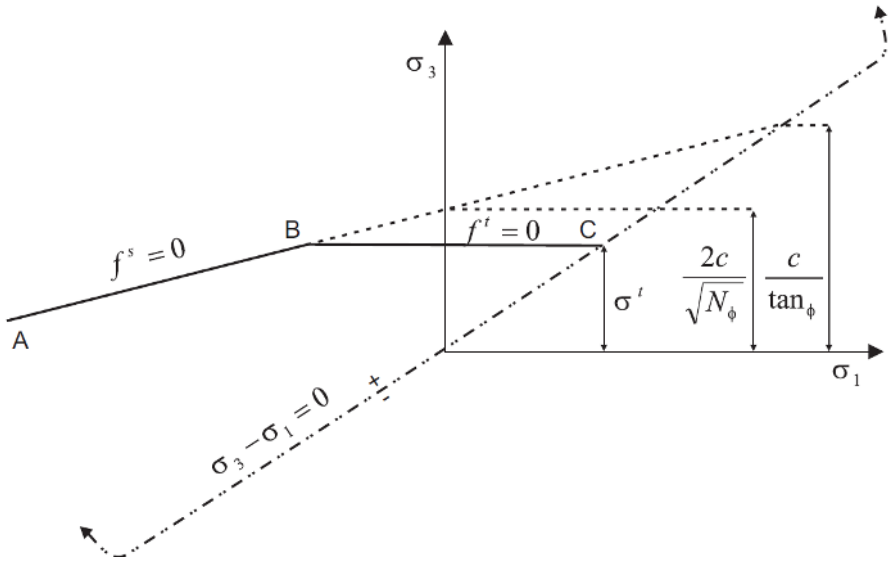

Figure 3: Mohr-Coulomb failure criterion used for plastic block behavior (Itasca 2018)

3 DEM of masonry structures subjected to in-plane and out-of-plane loading

3.1 Masonry wall panels subjected to combined shear and vertical pre-compression

The first study investigates the suitability of the model to predict the in-plane behaviour of a brickwork masonry wall panel subjected to combined shear and axial pre-compression. The developed numerical model compared against experimental test results obtained by testing two masonry wall panels (ZW1 and ZW2) made of concrete blocks and bonded together with mortar (Lurati et al 1990). The walls had dimensions equal to 3,600 mm × 2,000 mm × 150 mm (width × height × thickness) and were constructed by 10 rows of stretcher bonded concrete blocks. The dimensions of the blocks were 300 mm × 200 mm × 150 mm. Two partition walls were also attached at the ends of each of the main wall. The partition walls (ref. Figure 4a) had dimensions equal to 150 mm × 2,000 mm × 600 mm (width × height × thickness). Also, two concrete beams were positioned at the base and at the upper end of the wall to ensure an optimal transfer of the loading in the upper part and a fixed condition at the base. The three dimensional geometric model representing the masonry wall panels tested in the laboratory developed using 3DEC is shown in Figure 4b. To allow for the 10 mm thick mortar joints in the real wall panels, each masonry unit was based on the nominal brick size used in the laboratory built panels increased by 5 mm. Vertical pre-compression equal to 419 kN and 833 kN applied on the walls ZW1 and ZW2 respectively. An external horizontal load was also applied incrementally to the upper beam until the panel could no longer carry the applied load. The constitutive law to be used for representing the material behavior will affect the simulation results. The suitability of two different constitutive laws to represent the

behavior of the concrete block units were investigated. So, concrete blocks were modelled based on: a) a linear elastic behaviour; b) an elasto-plastic behaviour according to Mohr-Coulomb constitutive law. The mechanical properties for the block and mortar joints are shown in **Table 1** and **Table 2** respectively and are obtained from Lurati et al. (1990).

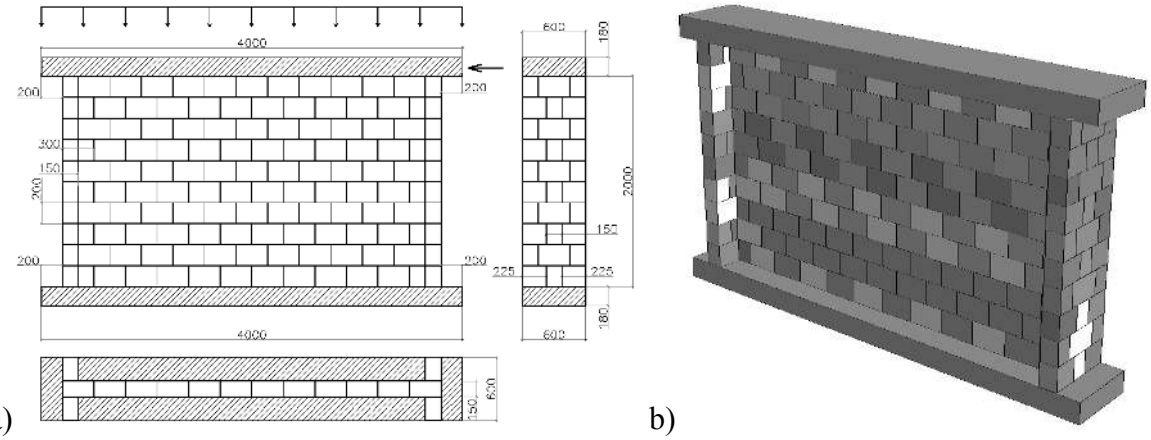

Figure 4: a) Geometry and application of load for ZW1 and ZW2 test panels (arrows denote the location of load and all units are in mm); b) Geometry of the model developed at 3DEC.

Table 1. Properties of the masonry units and the zero thickness interfaces; masonry blocks behave in a linear elastic manner.

Masonry block properties			Joint Interface properties					
Unit Weight [kg/m^3]	Bulk modulus [MN/m^3]	Shear modulus [MN/m^3]	Joint normal stiffness [MN/m^3]	Joint shear stiffness [MN/m^3]	Joint tensile strength [MPa]	Joint cohesive strength [MPa]	Joint friction angle [Degrees]	Joint dilatation angle [Degrees]
2,000	1.188E4	4.01E3	7.463E5	2.467E5	0.4	0.5	39	0

Table 2. Properties of the masonry units and the zero thickness interfaces; masonry blocks behave in an elasto-plastic manner based on the Mohr-Coulomb constitutive law.

Masonry blocks						Joint Interfaces					
Unit Weight [kg/m^3]	Bulk modulus [MN/m^3]	Cohesive Strength [MPa]	Tensile Strength [MPa]	Friction anlge [Degrees]	Dilation angle [Degrees]	Joint normal stiffness [MN/m^3]	Joint shear stiffness [MN/m^3]	Joint tensile strength [MPa]	Joint cohesive strength [MPa]	Joint friction angle [Degrees]	Joint dilatation angle [Degrees]
2,000	1.188E4	2.37	1.32	35	12	7.463E5	2.467E5	0.4	0.5	39	0

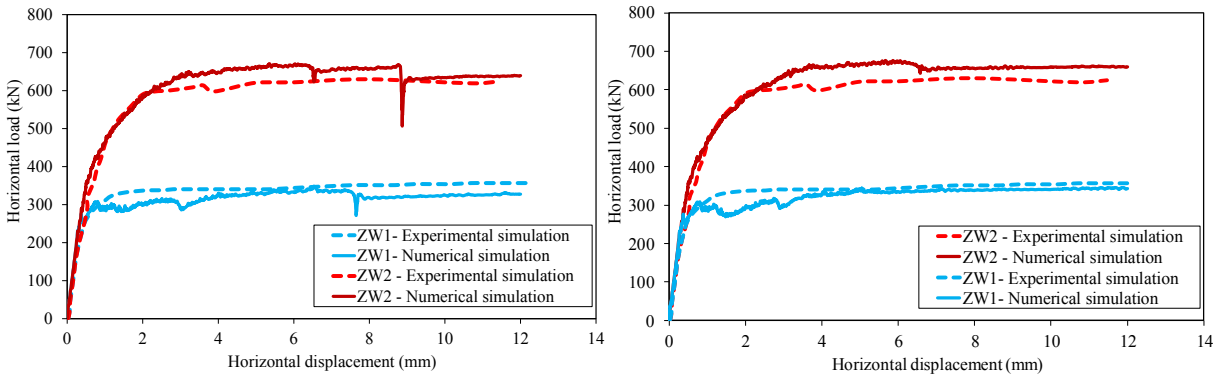

Figure 5: Load-displacement curves. Comparison of experimental results against those predicted by the numerical model: (a) blocks modelled as linear elastic; and (b) blocks modelled using the elasto-plastic Mohr Coulomb constitutive law.

Table 3. Comparison of experimental against numerical results

Test Wall	Ultimate load (kN)		Difference
	Experimental results	Numerical results	(%)
ZW1	353	346	1.98
ZW2	634	660	4.10

Figure 5 compares the experimental against the numerical results predicted using DEM. From the results analysis, and since failure is mainly at the brick-to-mortar interface, it is shown that both models are capable of predicting the load against horizontal displacement relationship for the wall panels ZW1 and ZW2 with adequate accuracy (maximum deviation is 4%; **Table 3**). In Figure 5a, the peaks in the post-cracking behavior indicate sudden crack formation and stress redistribution in the panel following cracking. Such behavior was not observed in the case where the blocks assumed as elasto-plastic. Instead, failure was dominated at the mortar joints rather than at the masonry blocks (**Figure 5b**).

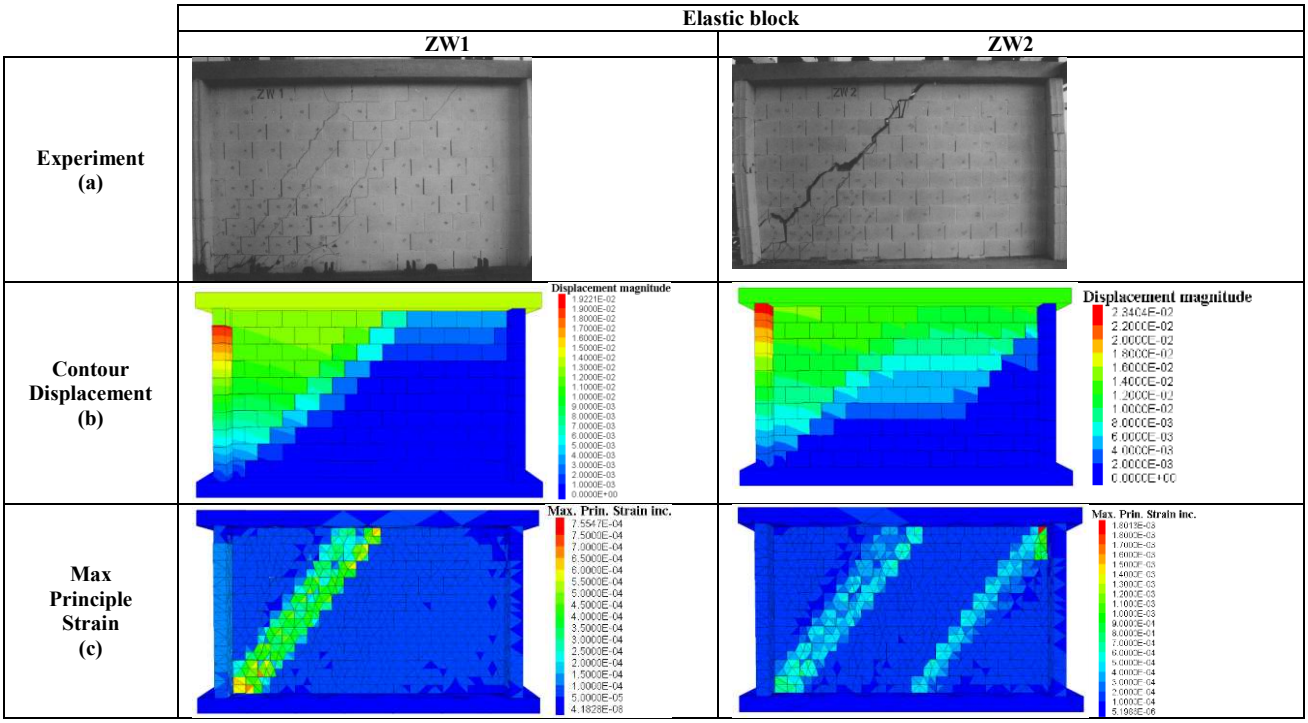

Figure 6: Comparison of experimental against numerical results based on the assumption that blocks behave in a linear elastic manner: a) Experimental failure mode; b) Numerical failure mode; c) Distribution of principal strain in the wall.

Experimental against numerical results were also compared qualitatively. The failure modes obtained by experimentally testing the ZW1 and the ZW2 wall panels were compared against the failure modes predicted from the numerical models taking into consideration the two different constitutive relationships used for representing the masonry blocks. From **Figure 6**a, during the experiment, a single diagonal crack run along the joints and blocks of the wall panel. However, the failure mode estimated by the numerical model under the assumption that the masonry block behaves in a linear elastic manner is dissimilar, since two diagonal cracks observed for the ZW2 test (**Figure 6**b and Figure 6c).

On the other hand, when the masonry block assumed to behave in an elastic-plastic behavior, a good agreement between the experimental and numerical failure mode was obtained (**Figure 7**). So, comparing the two different constitutive laws used to represent the mechanical behavior of masonry blocks, it was found that at very low levels of stress, a linear-elastic constitutive law is sufficient to simulate the mechanical behavior of masonry. Such type of masonry construction is that characterized by low bond strength i.e. where the masonry unit/mortar joint interface is sufficiently low to have a dominant effect on the mechanical behavior such as the formation of cracks, re-distribution of stresses after cracking and the formation of collapse mechanisms (Sarhosis 2012;

Sarhosis & Sheng 2014). However, at high stress levels, a nonlinear elastic-plastic model which can simulate crack formation, shear and/or crushing in the masonry blocks is required in order to more accurately reproduce the phenomena observed in the laboratory.

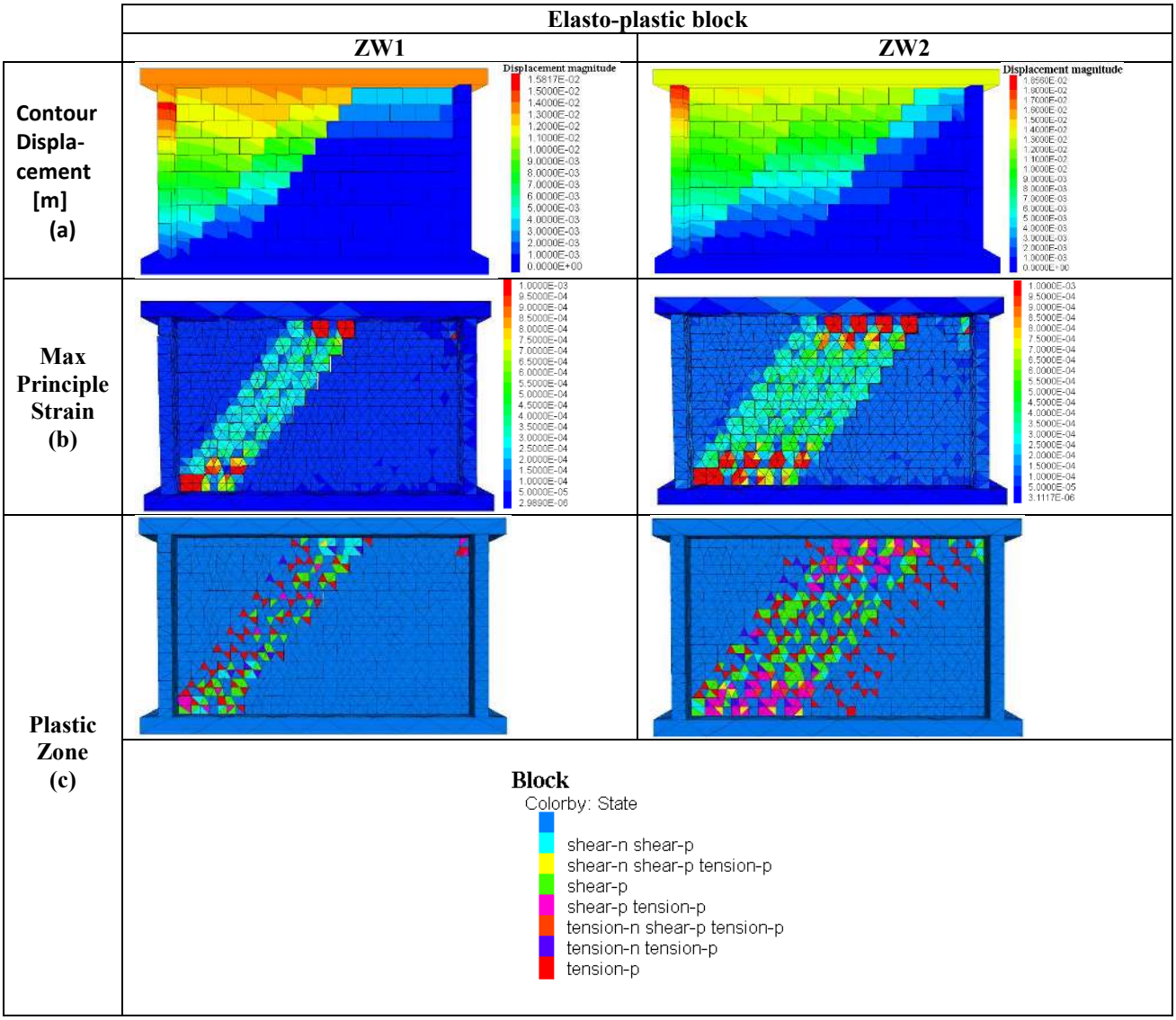

Figure 7: Comparison of experimental against numerical results based on the assumption that the blocks behave in an elasto-plastic behavior according to Mohr-Coulomb constitutive law: a) Numerical failure mode; b) Distribution of max principal strain in the wall; c) Plastic zone in the blocks

3.2 Out of plane loading

a) Solid rectangular masonry wall panels

The second case study deals with the development of a numerical model based on the DEM to study the out-of-plane behavior of a rectangular blockwork masonry wall panel. The developed numerical model was compared against experimental results obtained from the literature and reported at Gazzola et al. (1985). The mechanical behavior of three walls (WII, WP1 and WF) containing hollow concrete block units bonded with 10 mm mortar was studied. All walls were rectangular in shape with dimensions 5,000 mm × 2,000 mm (length × height). Also, walls were constructed with concrete block units' with dimensions equal to 190 mm × 390 mm × 150 mm (height × width × thickness). Panels WII and WP1 were supported on the four edges. Panel WF was supported on three edges while the top edge was left free. Also, for the panel WP1, an in-plane confining pressure equal to 0.2 N/mm^2 was assigned and kept constant during the experiment.

For the test-setup, a backup wall composed of plywood on a steel grid framework was tied back to the support frame to enclose the airbag placed between it and the test wall. The airbag was fabricated to cover the entire area of the wall. The 100 mm side pieces of the air bag matched the standard distance between the test wall and the backup wall. The air bag was inflated using a 690 kPa supply incorporating a pressure reduction valve and low pressure regulator on the intake. Lateral pressure was applied to all panels incrementally, with the use of airbags, until they could no longer carry any further load. The crack patterns obtained from the experimental study are shown in **Figure 8**.

a) 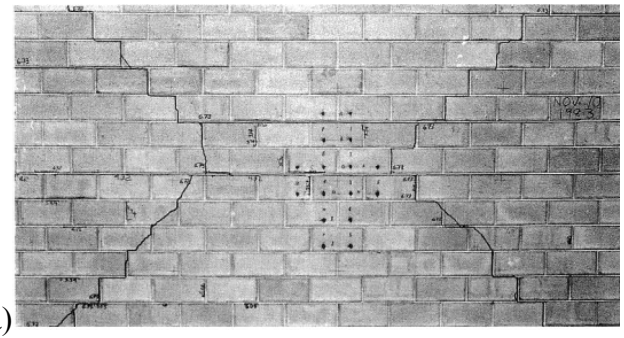 b) 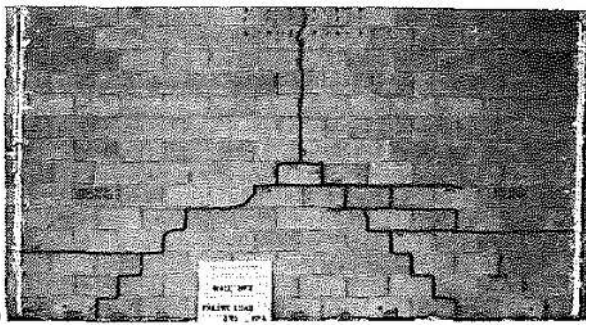

Figure 8: Crack patterns obtained from the experimental study: a) WII; b) WF (Gazzola et al. (1985).

Three dimensional geometric models representing the masonry wall panels tested in the laboratory were developed in 3DEC. To allow for the 10 mm thick mortar joints in the real wall panels, each masonry unit was based on the nominal brick size used in the laboratory built panels increased by 5 mm in each dimension to give a block size of 200 mm × 400 mm × 150 mm (height × width × thickness). It was assumed that the masonry units would exhibit linear elastic behavior

and that slip along the mortar joints would be the predominant failure mechanism. Mortar joints were represented using a Mohr-Coulomb failure surface combined with a tension cut-off. The material parameters used for the development of the computational models are shown in **Table 4**, whereas the material parameters used in the computational models are shown in Table 4. These values used by Gazzola et al., (1985) and Lourenco (1997) were proposed in their respective study after calibrating the overall stiffness of the wall (K = 4.744E6 Pa/m).

Table 5 compares the failure load for each panel obtained experimentally with the ones predicted by the numerical model based on the DEM. From **Table 5,** the DEM model can predict the ultimate load that the masonry wall panels can carry with sufficient accuracy. The values of the ultimate load predicted from the numerical model are close to the experimental results, with a maximum deviation of 5% for the WII wall panel.

Table 4. Properties of the masonry units and the zero thickness joint interfaces

Masonry unit properties		Joint Interface properties					
Young's modulus [N/m^2]	Poisson's ratio	Joint normal stiffness [Pa/m]	Joint shear stiffness [Pa/m]	Joint tensile strength [N/mm^2]	Joint cohesive strength [N/mm^2]	Joint friction angle [°]	Joint dilatation angle [°]
15,000	0.2	7.68E9	7.68E9	0.157	0.5966	36	0

Table 5. Comparison of experimental against numerical failure load

Wall	Experimental failure Load (kPa)	Numerical failure load by FEM (Lourenço, 1997)		Numerical failure load by DEM	
		Load (kPa)	Difference (%)	Load (kPa)	Difference (%)
WII	6,820	6,630	2.9	7,320	-5.0
WP1	8,820	9,720	-9.5	8,990	-1.9
WF	3,900	3,560	9.6	3,550	3.5

Figure 9 shows the failure mechanisms for the WII, WP1 and WF panels as obtained by the numerical model based on DEM. The experimental crack patterns are similar to those predicted by the yield line theory. The influence of in-plane normal pressure for the panels WII and WP1 is evident. From Table 5, it is also evident that the failure load increases with the confining pressure. This is due to the fact that the masonry wall panel is spanning in the direction where the normal

compressive stress is applied. Remarkably, the effect of in-plane action prevents horizontal cracks near the top and bottom of the panel WII (Figure 9).

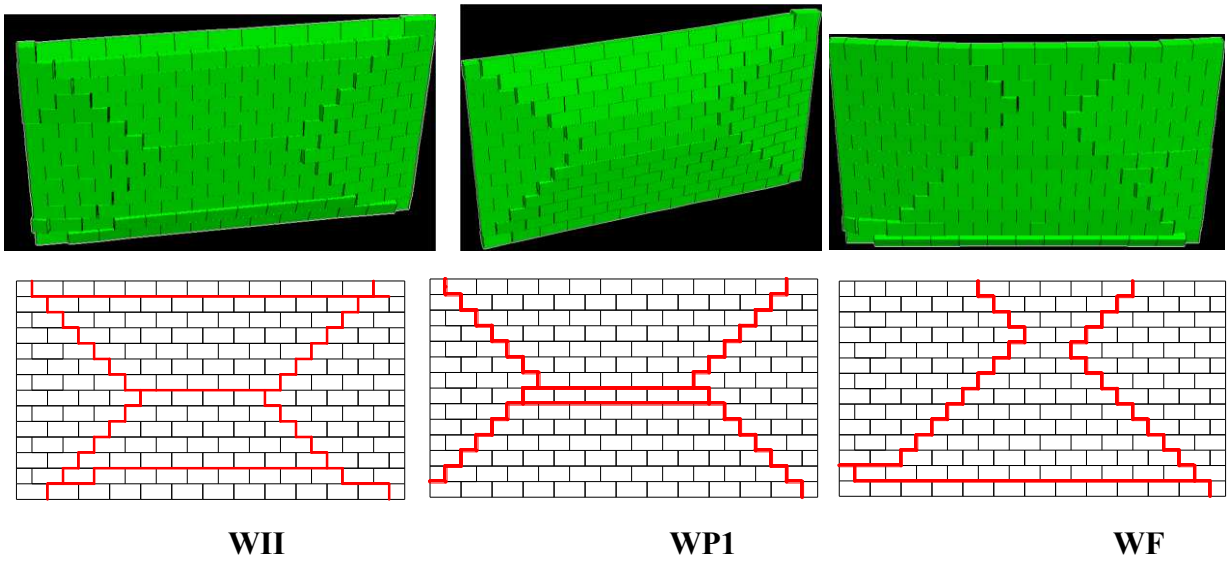

Figure 9: Failure mode obtained by DEM for the panels WII, WP1 and WF.

b) *Brickwork masonry wall panels containing an opening*

A numerical model was developed to simulate the mechanical behavior of the test wall SB02 containing a central opening. The numerical results were compared with those obtained from the experimental testing carried out by Chong et al. (1994). The dimensions of the wall were 5,600 mm × 2,475 mm × 102.5 mm (length × height × thickness). The central opening had dimensions of 2,260 mm × 1,125 mm × 102.5 mm (length × height × thickness). The SB02 test wall was constructed using bricks in stretcher bond with dimensions equal to 215 mm × 65 mm × 102.5 mm (height × width × thickness).The mortar joints were all nominally 10 mm thick.

The vertical edges were simply supported while the top edge left free. For the test-setup, the lateral load was generated by admitting compressed air into polythene bags sandwiched between the rear face of the panels and the steel reaction frame. Each bag was 2.475 m high by l.4 m width and was placed directly against the rear of the test panel, and against sheets of 12 mm thick plywood bearing onto the steel reaction frame. Timber beams were used to stiffen the plywood. A full scale 5.6 m length panel has been loaded by four airbags. The panels were loaded incrementally until failure. Load was applied in the out-of-plane direction of the masonry wall panels using airbags. Mid-span displacements on the top of the wall were recorded at all times. The crack patterns of the test wall SB02 obtained from the experimental study is shown in **Figure 10**. **Table 4** shows the

material parameters used in the developed computational models and adopted from Chong et al. (1994), Gazzola et al. (1985) and (Lourenço, 1997).

Figure 10: Crack patterns in the experimental study (SB02)

Figure 11a compares the experimental against the numerical load against mid-span displacement relationship as obtained from both the finite element method using a continuous model of elasto-plastic orthotropic type (Lourenço, 1997) and that of the discrete element method using the commercial software 3DEC. From Figure 10, both FEM and DEM models were able to predict the ultimate load with sufficient accuracy. **Figure 11**b shows the failure mechanisms obtained numerically using DEM. Also, from **Figure 11b**, the crack development at failure is in accordance with the one given by the yield line theory.

Table 6. Properties of the masonry units and the interfaces

Block		**Joint Interface**					
Young's modulus	Poisson's ratio	Normal stiffness	Tangent stiffness	Tensile strength	Cohesion	Friction angle	Dilatancy angle
[N/mm^2]		[Pa/m]	[Pa/m]	[N/mm^2]	[N/mm^2]	[°]	[°]
14,000	0.2	10E9	10E9	0.32	0.32	36	0

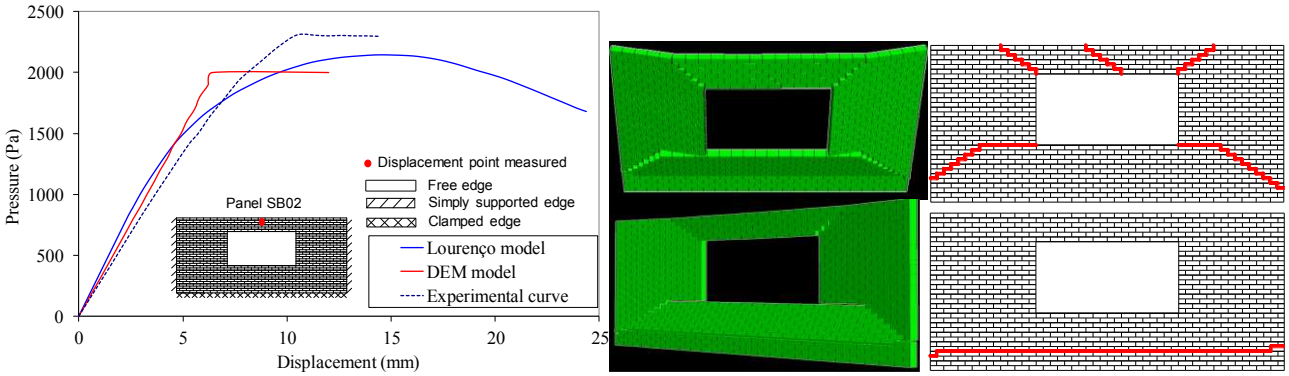

a) b)

Figure 11: Comparison of experimental against numerical results: a) Pressure against mid-span displacement relationship (SB02); b) Failure mode predicted by the numerical model.

c) Rectangular masonry wall panel connected with shear walls

The last case study deals with the simulation of two full scale rectangular masonry wall panels constructed with hollow concrete blocks running in a stretcher bonded blockwork and connected with two shear walls. The wall panels intended to represent the external face of a typical load-bearing wall. The top of the main wall was free to move, while the bottom and two sides were restrained. The main wall was 2,900 mm × 2,000 mm × 200 mm (length×width×height) and the two shear walls attached on the edges of the main wall had dimensions 1,500 mm × 2,000 mm × 200 mm. Horizontal steel reinforcement (3 bars with a 6mm diameter) was installed on the top end of the wall. Also, a vertical steel reinforcement (2 bars with a 12mm diameter) was installed at each corner, in accordance with the constructive process and standards (EN 1996-1-1, 2005). Only the masonry block units which contained steel reinforcement were filled with concrete. For the test-setup, the main wall was subjected to a quasi-static loading of uniform pressure applied to the outside face by six inflatable cushions or water bags (**Figure 12**). The reaction wall (a reaction frame) consisted of a set of metal HEB beams, anchored on the laboratory test slab by pre-stressed steel bars (Bui, 2014b).

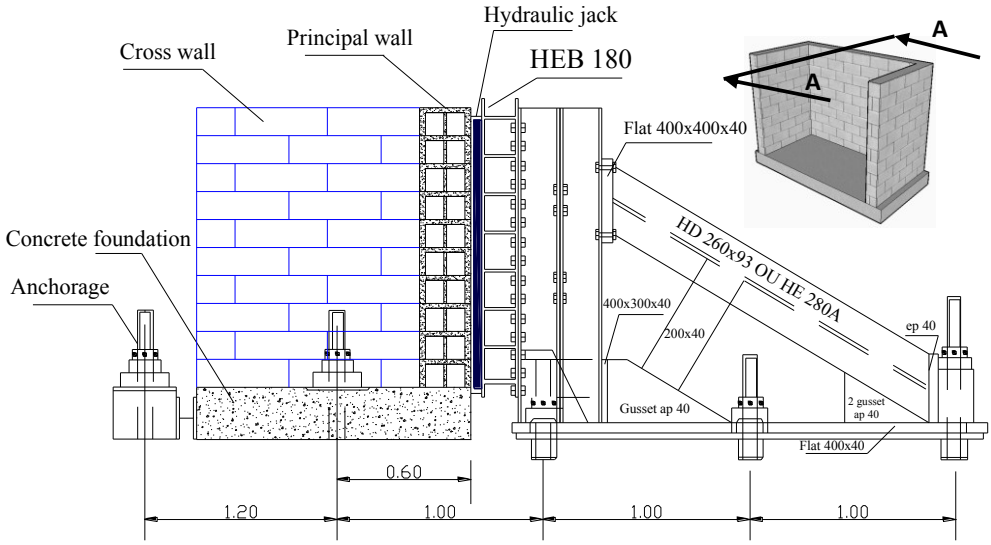

Figure 12: Experimental test arrangement

Three-dimensional discrete element models of the masonry structure tested in the laboratory were developed in 3DEC software (**Figure 13**b). Each block of the wall had dimensions equal to 500 mm x 200 mm x 200 mm (length × width × height). The bottom part of the walls was fixed in all directions. The block and zero thickness interface parameters used for the development of the computational model were obtained from (Bui et al., 2014b; Bui, 2013) and are shown in **Table 7** .

Horizontal and vertical reinforcement was modelled using 1D elements assuming to behave in an elastic perfectly plastic manner (**Figure 13**c). The 1D element allows the modelling of a shearing resistance along their length, as provided by the shear resistance (sbond) between the grout. The cable element was divided into a number of segments of equal in size lengths and passed through the joints, with nodal points located at each end of the segment. Shearing resistance was represented by spring/slider connections (kbond/sbond) between the structural nodes and the block zones in which the nodes are located. The tensile yield strength of steel reinforcement was taken equal to 400 MPa. A high grout shear stiffness and cohesive strength was assigned to the 1D element nodes; since reinforcement was embedded in the masonry wall. The bond beam at the top of the walls contained three 6 mm diameter reinforcing elements. The vertical reinforcement elements (2 bars with a 12 mm diameter) were placed at each corner of the wall. First, the numerical model was brought into equilibrium state under its own self-weight. Then, a controlled pressure was assigned to the masonry wall specimen. The load-deflection curve obtained numerically is relatively similar to the one obtained experimentally (**Figure 14**). Also, good agreement between the numerical and experimental cracking patterns obtained (**Figure 15**).

Table 7. Properties of the masonry units and the interfaces

Block			Interface					
Density	Bulk modulus	Shear modulus	Normal stiffness	Shear stiffness	Tensile strength	Cohesion	Friction angle	Dilatancy angle
[kg/m^3]	[MPa]	[MPa]	[Gpa/m]	[Gpa/m]	[N/mm^2]	[N/mm^2]	(°)	(°)
2,500	3,200	2,700	14	14	0.3	0.45	48	36

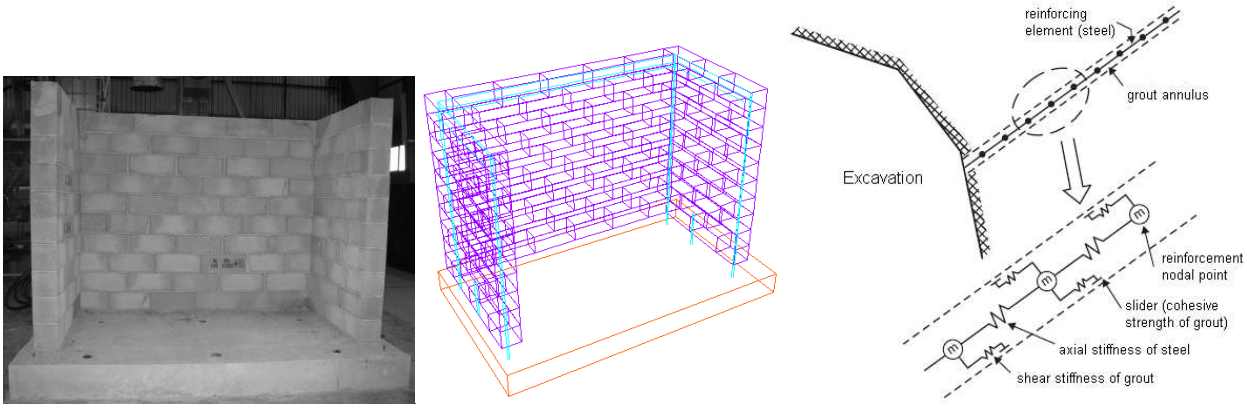

a) b) c)

Figure 13: a) Geometry of the masonry structure tested in the laboratory; b) Development of the computational model using 3DEC (cable modelling in blue colour); c) Representation of the one-dimensional reinforcing element in DEM.

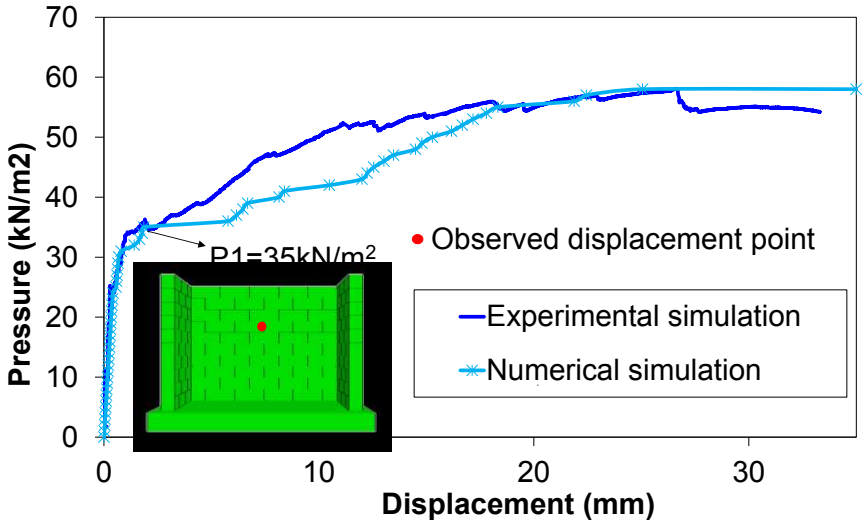

Figure 14: Comparison of experimental and numerical pressure against mid-span displacement relationship

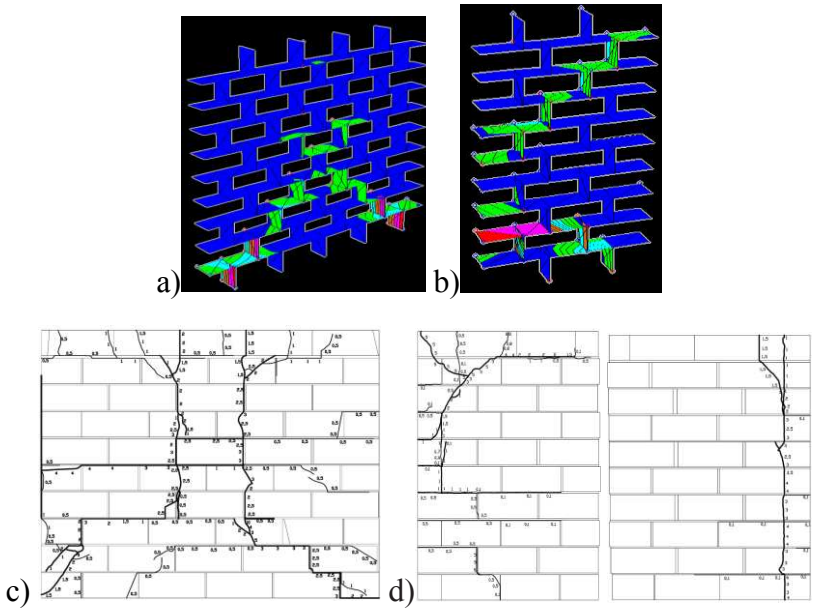

Figure 15: a) b) DEM: Fracture surface in the joint interface (principal wall and return wall); c) d) failure mode obtained in experimental simulation (main wall and shear wall).

d) Parametric study: geometric ratio and boundary conditions effects

A parametric study to investigate the influence of: a) the geometric ratio length over height (L/H) of the panels; and b) the influence of the boundary conditions on the ultimate load carrying capacity of the walls subjected to out-of-plane loading was undertaken. Geometric models representing the masonry wall panels WII (fixed at four edges) and WF (fixed at three edges) tested in the laboratory by Gazzola et al. (1985) were developed in the numerical model based on the DEM. To allow for the 10 mm thick mortar joint in the real wall panels, each masonry unit was based on the nominal brick size used in the laboratory built panels increased by 5 mm in each direction to give a block size equal to 190 mm × 390 mm × 150 mm (height × width × thickness). The ration of the L/H varied from 0.43 to 4.29 but the height (H) of the wall was kept constant and equal to 2,000 mm. It was assumed that the bricks would exhibit linear elastic behavior and that slip along the mortar joints would be the predominant failure mechanism. The material properties for the mortar joint interface are shown in **Table 4**. Also, the normal and shear stiffnesses were kept constant and equal to 7.68×10^9 Pa/m. Load in the form of a uniform pressure was applied incrementally in the structure until collapse occurred. **Figure 16** illustrates the relationship between failure loads against the length over height ration for the different boundary conditions studied. From **Figure 16**, as the L/H increases, the load carrying capacity of the masonry wall panel reduces. Furthermore, for L/H greater than 2.25, the ultimate load that the masonry wall panel can carry is almost constant. A

remarkable increase in the ultimate load carrying capacity was observed when the L/H was less than 1. Similar results were also obtained from Essawy (2004) using numerical models developed based on the FEM. Such findings are consistent with the theory of the yield lines (Johanson, 1972). The behavioral tendency in the case of the masonry wall panel fixed at three edges is similar to that observed in the case of the masonry wall panel fixed at four edges. However, by changing the boundary condition in the wall panel from four to three fixed edges, decreased from 10% to 50% the ultimate load that the panel can carry.

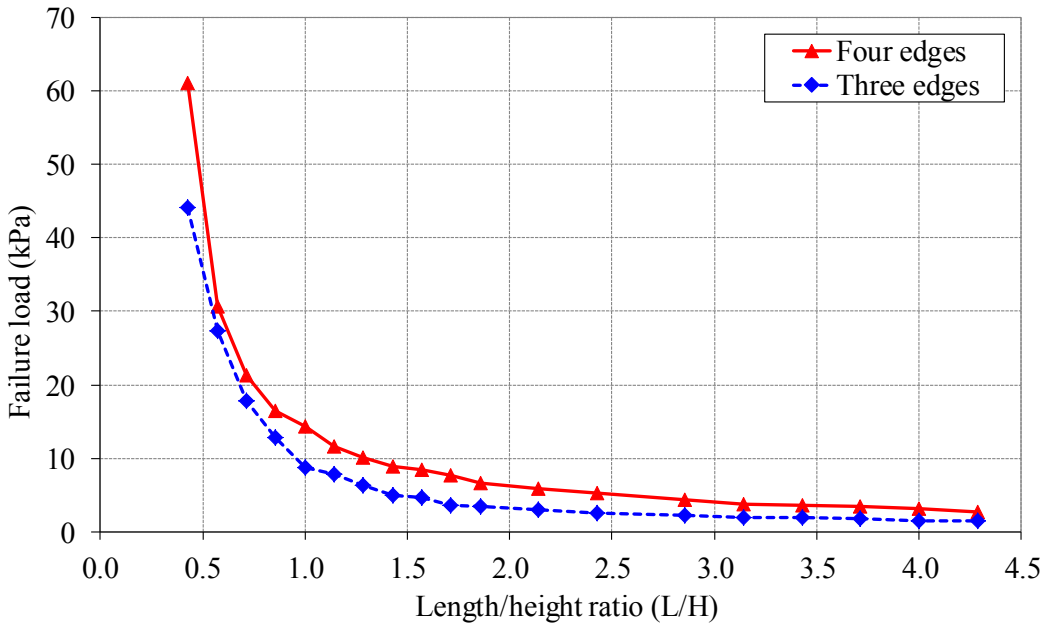

Figure 16: Influence of geometric properties and boundary conditions on the load carrying capacity of the masonry wall panel.

4 Conclusions

Today, a wide variety of numerical methods have been developed in the literature to simulate the mechanical behavior of masonry structures. The choice of the most appropriate tool for the analysis of masonry structures requires a good understanding of both the constitutive model and the input material properties to be selected by the modeler. This article evaluates the efficiency and performance of the discrete element method to simulate the mechanical behavior of different masonry wall panels subjected to in-plane and out-of-plane loading. The assessment consisted of a comparison of the results from full-scale laboratory tests to the behaviour predicted using the discrete element modelling software, 3DEC. More specifically, the suitability of the model is based on its ability to predict the development and propagation of cracks up to collapse, the associated stress distributions in the wall panels at different magnitudes of the applied loading and the ultimate load carrying capacity.

From the results analysis, it was found that the heterogeneous nature of masonry and the discontinuity at block interfaces can be well described by a discrete element approach. The numerical simulations were in good agreement with experimental results. In particular, the conducted simulations allowed us to quantify with sufficient accuracy the bearing capacity of the structures as well as the cracking initiation and propagation. In addition, the nonlinear behavior observed in the experimental load-deflection curves were globally correctly reproduced from the initiation up to the final failure. This, traduces that crack appearance and propagation, were correctly reproduced. Stress redistributions inherent to cracks were also well represented, which allowed us to identify areas of potential crack propagation and to predict the failure mechanism traducing the correct estimation of the bearing capacity as well as the characterization of the collapse mode of the structure.

Difficulties in the choice of input parameters arise mostly due to the shortage of experimental data, the proper characterization of the masonry material constituents (blocks and mortar) and the masonry specimen. On the other hand, there is still a challenge to discontinuous idealizations for large and complex geometrical structures, as it is essential to simplify them. However, this requires experience and a good insight in the expected structural behavior.

For masonry structures, the DEM allows to simulate rupture phenomena taking into account the discontinuous nature of masonry in an elegant and robust way.

References

A. Munjiza, “The combined finite-discrete element method”, New York: Wiley, 2004.

A.W. Hendry, B.P. Sinha, S.R. Davies, “Design of masonry structures”, London: E&FN Spon, 2004.

Andreaus, U., Casini, P., Dynamics of three-block assemblies with unilateral deformable contacts. Part 1: Contact modelling, Earthquake Engineering and Structural Dynamics, Volume 28, Issue 12, December 1999a, Pages 1621-1636.

Andreaus, U., Casini, P., Dynamics of three-block assemblies with unilateral deformable contacts. Part 2: Actual application, Earthquake Engineering and Structural Dynamics, Volume 28, Issue 12, December 1999b, Pages 1637-1649.

Bui T.T, Limam A, Bui Q B. “Characterization of vibration and damage in masonry structures: experimental and numerical analysis”. *European Journal of Environmental and Civil Engineering,* 2014a.

Bui T.T. “Masonry walls submitted to out-of-plane loading: experimental and numerical study”. *PhD Thesis, INSA Lyon*, 2013, http://www.sudoc.fr/183858298

Bui T.T, Limam A. Out-of-plane behaviour of hollow concrete block masonry walls unstrengthened and strengthened with CFRP composite. Composites Part B: Engineering, Volume 67, December 2014b, Pages 527-542, 2014

Bui T.T, Limam A, Sarhosis V, Hjiaj M. 2017. Discrete element modelling of the in-plane and out-of-plane behaviour of dry-joint masonry wall constructions. Engineering Structures, 136, 277-294.

Chong, V.L. Southcombe, C., and May, I.M. (1994). “The behaviour of laterally loaded masonry panels with openings.” Proc., 3rd Int.

Colas A.S., Mechanical modeling of dry stone retaining walls by calculation at failure and experimentation scale 1”, PhD Thesis, ENTPE, Vaulx-en-Velin, 2009.

Cundall P. A., A computer model for simulating progressive, large scale movements in blocky rock systems, Proc. Int. Symp. Rock Fracture, ISRM, Nancy, Vol. 1, Paper II–8, 1971a.

Cundall P. A., “The measurement and analysis of acceleration in rock slopes”, Ph.D. Thesis, Imperial College of Science and Technology, University of London, 1971b

E.A. Gazzola, R.G. Drysdale, A.S Essawy. Bending of concrete masonry walls at different angles to the bed joint. Proc. 3rd North. Amer. Mas. Conf., Arlington, TX, USA, Paper 27, 1985.

Essawy, A. S., “Strength of Block Masonry Walls Subject to Lateral Loading”, Thèse de doctorat, McMaster University.

EN 1996-1-1. 2005. “Design of masonry structures. Part 1-1: general rules for reinforced and unreinforced masonry. ” CEN, Brussels.

Forgács T, Sarhosis V, Bagi K. Minimum thickness of semi-circular skewed masonry arches. Engineering Structures, 140(1), 317–336, 2017.

Forgács T., Sarhosis V., Bagi K., Influence of construction method on the load bearing capacity of skew masonry arches. Engineering Structures, 168, 612-627, 2018.

Gazzola E.A., Drysdale R.G., “A component failure criterion for blockwork in flexure”, Proc., Structures ASCE, S.C. Anand, ed., New Orleans, 134-153, 1986.

Giamundo V., Sarhosis V., Lignola G.P., Sheng Y., Manfredi G. Evaluation of different computational modelling strategies for modelling low strength masonry, Engineering Structures, 201473, 160-169. DOI: 10.1016/j.engstruct.2014.05.007

Itasca, 3DEC – Three Dimensional Distinct Element Code, Version 6.0, Itasca, Minneapolis, 2018.

J.G. Rots, “Structural masonry: an experimental/numerical basis for practical design rules”, Rotterdam: Balkema, 1997.

Johansen, K.W., “Yield-line formulae for slabs, Cement and Concrete Association”, London, 1972.

Kelman I., Spence R., “A Limit Analysis of Unreinforced Masonry Failing Under Flood Water Pressures”, Masonry International, vol. 16, no. 2, 51-61, 2003.

Lemos J.V., “Discrete Element Modeling of Masonry Structures”, International Journal of Architectural Heritage, 1:190-213, 2007.

Lofti H.R., Shing P.B.: “An appraisal of smeared crack models for masonry shear wall analysis”, Computer and Structure, vol.41, issue 5, 413-425, 1991.

Lurati F., Thürlimann B., “Tests in concrete masonry walls (in German)”, Report No. 8401-3, Institute of Structural Engineering, ETH Zurich, Zurich, Switzer-land, 1990.

Lourenço, P.B. “Aspects related to the out-of-plane numerical modeling of masonry”, Mas Int, 14:31–4, 2000.

Lourenço P.B., Rots J.G., “Multisurface interface model for analysis of masonry structures”, ASCE J. Eng Mech, 123:660–8, 1997.

Lourenço P.B.. Computational strategies for masonry structures. PhD Thesis, Delft University of Technology, the Netherlands, 1996.

Lourenço P.B.,. An anisotropic macro-model for masonry plates and shells: Implementation and validation. Rep. No. 03.21.1.3.07, Univ. of Delft, Holland and Univ. of Minho, Guimaraes, Portugal, 1997.

Moradabadi, E., Laefer, D. Opportunities in Numerical Modelling of Pre-existing Damage of Historical Masonry Buildings (paper 1600). In 9th International Masonry Conference Guimarães, Portugal. 2014.

Rots J.G., Nauta P., Kusters G.M.A., Blaauwendraad J., “Smeared crack approach and fracture localization in concrete”, Heron, 30(1), p.3-48, 1985.

Sarhosis V., Garrity S.W., Sheng Y. Influence of the brick-mortar interface on the mechanical response of low bond strength masonry lintels, Engineering Structures, 2015. 88, 1-11. DOI: 10.1016/j.engstruct.2014.12.014

Sarhosis V., Oliveira D.V., Lemos J.V., Lourenco P. The effect of the angle of skew on the mechanical behaviour of arches, Journal of Mechanics Research Communications, 2014a. 61, 53-49. DOI: 10.1016/j.mechrescom.2014.07.008.

Sarhosis V. Computational modelling of low bond strength masonry. PhD thesis. University of Leeds, UK. 2012.

Sarhosis V., Sheng Y. Identification of material parameters for low bond strength masonry, Engineering Structures, 2014. 60, 100-110. DOI: 10.1016/j.engstruct.2013.12.013.

Sarhosis V., Tsavdaridis K., Giannopoulos G. Discrete Element Modelling of masonry in-filled steel frames with multiple window openings subjected to lateral load variations, Open Construction and Building Technology Journal, 2014b. 8(1), 93-103.

Sarhosis V., Lemos J.V. Detailed micro-modelling of masonry using the discrete element method. Computers and Structures, 2018. 206, 66-81.

Thomas K., "Structural Brickwork – materials and performance", The Structural Engineer, 49 (10). 441 – 450, October 1971.